HI absorption spectra for Supernova Remnants in the VGPS survey

Denis Leahy and Sujith Ranasinghe
University of Calgary, Calgary, Canada

The Current Study

- Sample: supernova remnants (SNR) from Green's SNR catalog which are found in the VLA Galactic Plane Survey region
- The 34 SNR are listed in Table 1
- 1420MHz radio continuum data and HI line data were obtained from the VLA Galactic Plane Survey (Stil et al, 2006)
- $^{13}CO(J = 1\text{-}0)$ data are from the Galactic Ring survey (Jackson et al 2006)
- HI absorption spectra were made according to the method of Leahy & Tian (2010).

Table 1: *Supernova remnants*

#	Source	Kilpatrick (kpc)	Green (kpc)	Other (kpc)
01	G18.1 -0.1	5.6	4^{A}	Leahy (2014), Paron (2013)
02	G18.6 -0.2	13.2	-	-
03	G18.8 +0.3	-	12	12.1 Tian (2007) 6.9-15 kpc
04	G18.9 -1.1	-	2	2 Fürst (1989)
05	G20.0 -0.2	-	-	-
06	G20.4 +0.1	-	-	-
07	G21.5 -0.9	4.8	4.6	4.8 Tian (2008)
08	G21.8 -0.6	-	5.2	5.5 Tian (2008), 5.2 Xin (2009)
09	G22.7 -0.2	-	-	3.7 Anderson (2011)
10	G23.3 -0.3	-	4.2	4.1 Leahy (2008)
11	G23.6 +0.3	6.9	-	-
12	G24.7 -0.6	-	-	-
13	G24.7 +0.6	-	-	$\leq$ 5.25 Clark (2003), 3.5/12 Petriella (2012)
14	G27.4 +0.0	8.5	7.5-9.8	7.5-9.8 Tian (2008)
15	G27.8 +0.6	-	-	Maybe 2-3 Misanovic (2010), Reich (1984)
16	G28.6 -0.1	-	-	Maybe 6-8.5 Bamba (2001) or 7
17	G29.6 +0.1	10.0	-	10 Gaensler (1999)
18	G29.7 -0.3	6.0	11.0	5.1-7.5 Leahy (2008), 10.6 Su (2009)
19	G31.9 +0.0	7.2	8.5^{T}	7.2-11.4 Radhakrishnan (1972)
				7.2 Su (2013), 5.4 Park (2013)
20	G32.8 -0.1	-	4.8^{C}	4.8 Zhou(2011), 4.6 Park (2013)
21	G33.6 +0.1	7.1	7.8	7.1 Case (1998), 7.8 Green (2004), 5.1 Park (2013)
22	G34.7 -0.4	-	2.8	$<$ 3.3 Su (2013), 3 Caswell (1975), 2.8 Park (2013)
23	G35.6 -0.4	-	-	12 Philips (1993), 10.5 Han (2006), 3.6
				(3.6/10.2) Zhu (2013), 7.6 Park (2013)
24	G39.2 -0.3	6.2	> 7.7	6.2-12.5 Su (2011), 8 Anderson (2011), 6.5 Hewitt (2009)
25	G41.1 -0.3	10.3	> 7.5	Leahy and Ranasinghe (2016), 6.1 Park (2013)
26	G41.5 +0.4	-	-	-
27	G42.0 -0.1	-	-	-
28	G43.3 -0.2	12.5	10.0	12.5 Lockhart (1978), 10/8 Moffett (1994), 4.8 Park (2013)
29	G45.7 -0.4	-	-	9.1 Park (2013)
30	G46.8 -0.3	-	6.8-8.6	6.8-8.6 Sato(1979), 5.8 Park (2013)
31	G49.2 -0.7	-	$6^{C}/4.3^{H}$	6 Koo (1995)/ 4.3 Tian (2013), 1.9 Park (2013)
32	G54.1 +0.3	6.2	$8^{C}/4.5-9^{H}$	6.2 or 4.5-9 Leahy (2008), 8.2 Lee (2012)
33	G54.4 -0.3	-	-	3.3 Case (1998), 3.7 Park (2013)
34	G57.2 +0.8	8.2	-	14.3 Park (2013)

Superscripts A: Associated with other sources, C: CO indicates distance H: HI indicates distance, T: Absorption up to the Tangent point

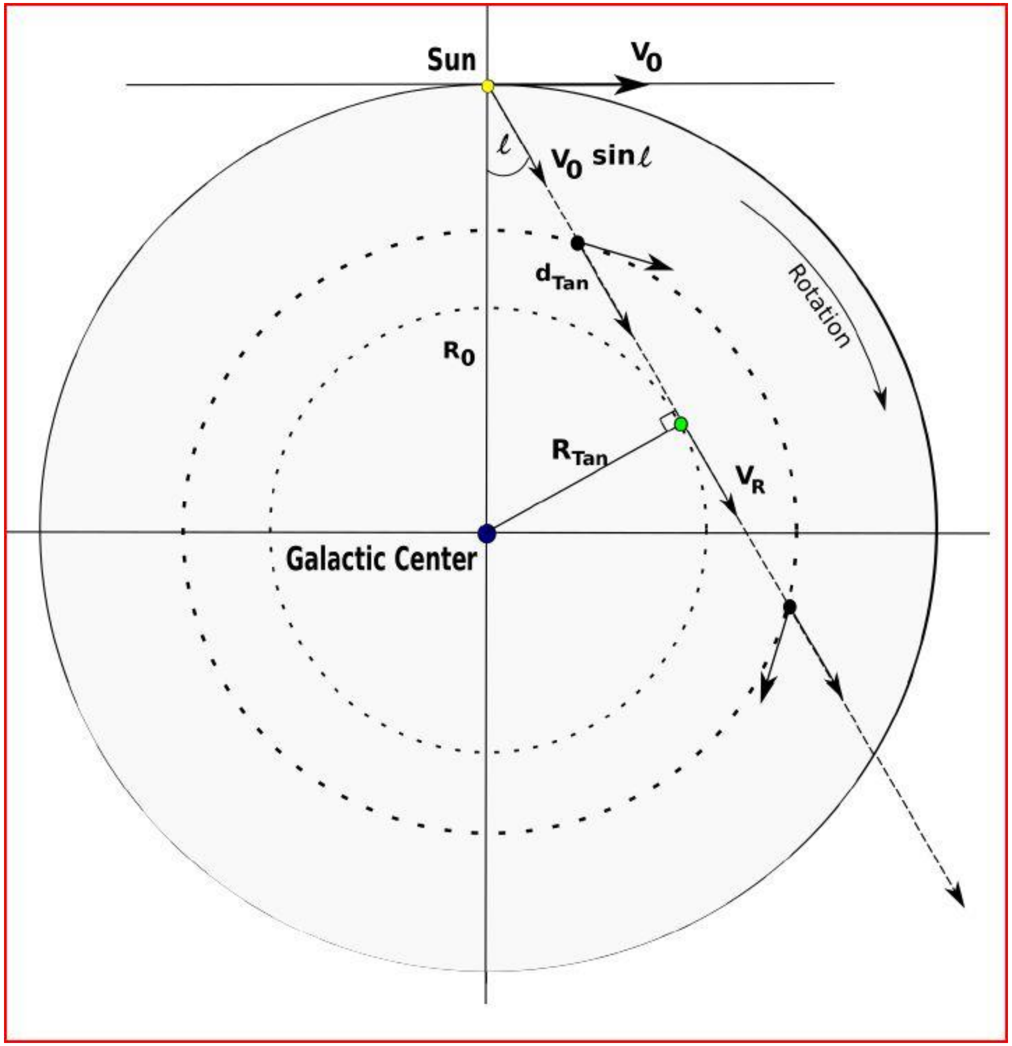

Schematic top-down view of the Galactic plane illustrating:
the solar circle;
The line of sight in a given direction in the first quadrant;
the position of the tangent point;
nearside gas moving at Vr<Vtan;
farside gas moving at Vr<Vtan.

We measure the rotation curve in the inner Galaxy by measuring the HI emission spectra toward the 34 SNRs to extract the velocity of the highest velocity peak and the maximum velocity where the HI intensity drops to zero.

Table 2: *Supernova remnants*

#	Source	$V_{r,tan}1$ (km/s)	$V_{r,tan}2$ (km/s)	$V_{r,tan}3$ (kpc)	d_{tan} (kpc)	R_{min} (km/s)
01	G18.1 -0.1	202.728	192.728	205^{+1}_{-1}	7.918	2.588
02	G18.6 -0.2	204.533	194.533	203^{+1}_{-1}	7.895	2.657
03	G18.8 +0.3	205.254	190.254	203^{+3}_{-4}	7.886	2.684
04	G18.9 -1.1	205.614	195.614	205^{+1}_{-1}	7.881	2.698
05	G20.0 -0.2	204.560	194.560	205^{+2}_{-2}	7.827	2.849
06	G20.4 +0.1	205.989	195.989	206^{+1}_{-1}	7.808	2.904
07	G21.5 -0.9	209.897	209.897		7.750	3.053
08	G21.8 -0.6	210.958	195.958	208^{+2}_{-2}	7.734	3.093
09	G22.7 -0.2	209.128	194.128	210^{+2}_{-3}	7.685	3.215
10	G23.3 -0.3	213.229	196.229	210^{+4}_{-4}	7.651	3.295
11	G23.6 +0.3	217.276	197.276	214^{+1}_{-1}	7.633	3.335
12	G24.7 -0.6	216.095	191.095	215^{+1}_{-2}	7.568	3.481
13	G24.7 +0.6	216.095	201.095	215^{+1}_{-1}	7.568	3.481
14	G27.4 +0.0	210.324	200.324	218^{+1}_{-1}	7.396	3.833
15	G27.8 +0.6	211.672	211.672	218^{+2}_{-2}	7.369	3.885
16	G28.6 -0.1	224.355	209.355	217^{+3}_{-4}	7.314	3.988
17	G29.6 +0.1	227.679	212.679	226^{+3}_{-3}	7.243	4.114
18	G29.7 -0.3	228.010	213.010	226^{+3}_{-3}	7.236	4.127
19	G31.9 +0.0	230.200	220.200	236^{+5}_{-3}	7.072	4.402
20	G32.8 -0.1	233.092	218.092	235^{+3}_{-3}	7.002	4.512
21	G33.6 +0.1	235.639	215.639	242^{+3}_{-4}	6.938	4.610
22	G34.7 -0.4	229.103	209.103	238^{+4}_{-8}	6.848	4.742
23	G35.6 -0.4	226.903	211.903	237^{+3}_{-3}	6.773	4.849
24	G39.2 -0.3	237.782	222.782	239^{+3}_{-3}	6.455	5.265
25	G41.1 -0.3				6.277	5.476
26	G41.5 +0.4	229.451	204.451	235^{+3}_{-3}	6.239	5.520
27	G42.0 -0.1	230.870	210.870	237^{+5}_{-5}	6.190	5.574
28	G43.3 -0.2	229.508	219.508	240^{+4}_{-5}	6.062	5.713
29	G45.7 -0.4	238.021	221.021	240^{+4}_{-4}	5.818	5.962
30	G46.8 -0.3	238.915	218.021		5.702	6.072
31	G49.2 -0.7	245.025	225.025	248^{+3}_{-3}	5.443	6.306
32	G54.1 +0.3	241.589	223.589	248^{+3}_{-3}	4.884	6.748
33	G54.4 -0.3	242.256	217.255	247^{+5}_{-5}	4.849	6.773
34	G57.2 +0.8	240.244	218.244	244^{+4}_{-4}	4.512	7.002

Additionally we model the HI emission spectra using a given rotation curve and a Gaussian velocity dispersion for the HI. We find good agreement with the rotation curve given in Reid et al (2014 ApJ 783,130) which uses the form derived by Persic et al 1996 (MNRAS, 281, 27)

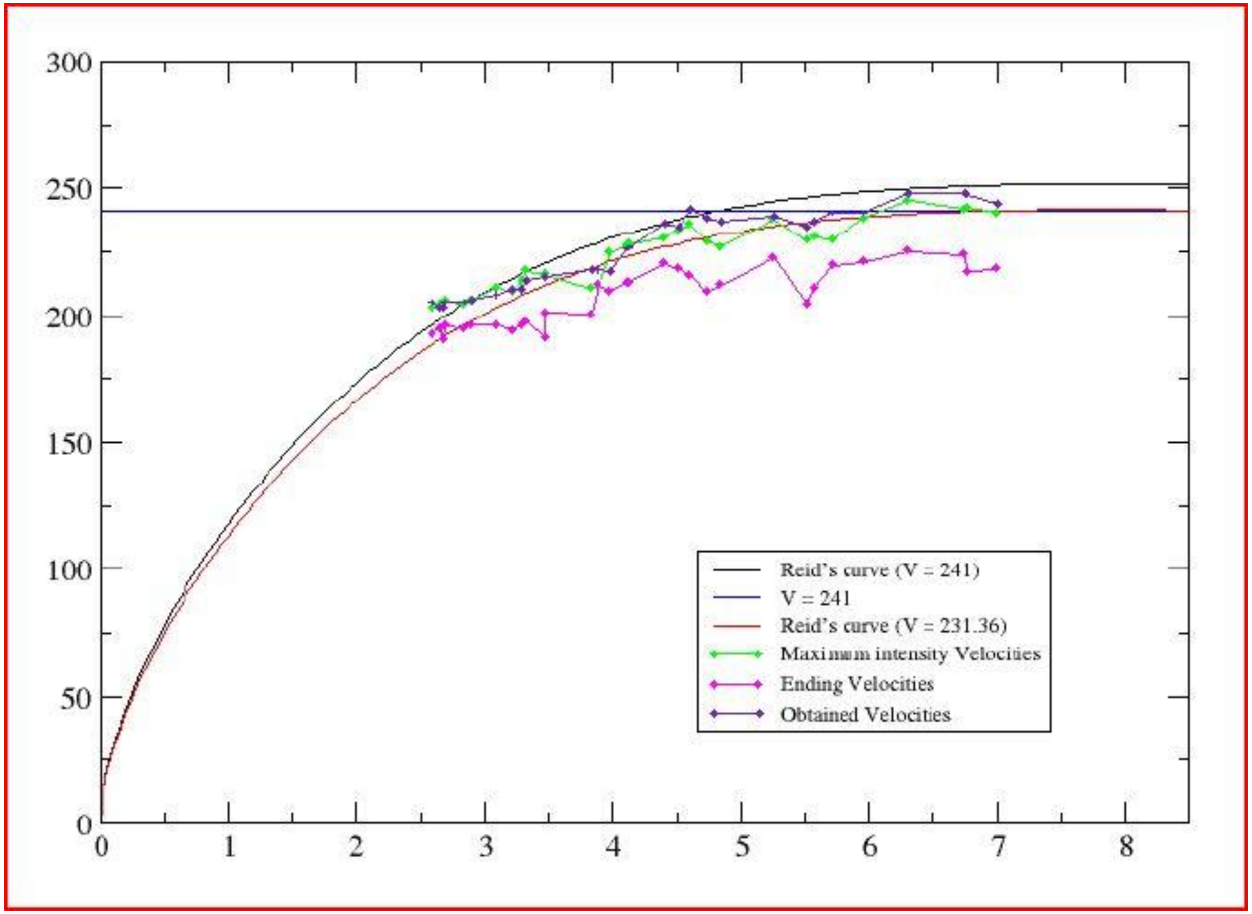

Derivation of HI absorption spectra

The solution of the equation of radiative transfer for plane parallel geometry (which holds generally if scattering can be ignored) is:

$$I_\nu(0) = I_\nu(\tau_0)e^{-\tau_0} + \int_0^{\tau_0} S_\nu(\tau)e^{-\tau}d\tau \tag{4}$$

This is then converted to brightness temperature(T_B) units using $I_\nu = 2k_B T_B(\mathrm{v})/\lambda^2$ where $T_B(\mathrm{v})$ has label v, the radial velocity corresponding to the frequency shift caused by the velocity of the HI along the line-of-sight. The result is then put into discrete form using an arbitrarily large set of optically thin HI clouds and of optically thin continuum emission regions:

$$T_B(\mathrm{v}) = \sum_{\mathrm{m=0}}^{\mathrm{m_c}} \mathrm{T^c_{B,m}e^{-\tau_m(v)}} + \sum_{\mathrm{n=0}}^{\mathrm{n_{HI}}} \tau^{(\mathrm{n})}(\mathrm{v})\mathrm{T_{B,n}(v)e^{-\tau_n(v)}} \tag{5}$$

where the index m sums over emission regions and the index n sums over emitting and absorbing HI clouds. Here $\tau_m(v)$ and $\tau_n(v)$ are the total opticals depth (at the frequency corresponding to velocity v) from each continuum or HI region to the observer, whereas $\tau^{(n)}(\mathrm{v})$ is the optical depth of a single HI region along the line-of-sight.

In order to construct the HI absorption spectrum for our continuum region of interest, the spectrum from the background line-of-sight is subtracted from the one for the line-of-sight through the source. For two adjacent lines-of-sight (1 and 2), with the only difference is a single continuum emission region, j, the resulting spectrum is:

$$T_B(v,1) - T_B(v,2) = (T^c_{B,j,1} - T^c_{B,j,2})e^{-\tau_j(\mathrm{v})} \tag{6}$$

For the case that the data have T_B defined with a continuum image at a nearby frequency subtracted (using velocity channels free of HI absorption) the result is instead:

$$T_B(v,1) - T_B(v,2) = (T^c_{B,j,1} - T^c_{B,j,2})(e^{-\tau_j(\mathrm{v})} - 1) \tag{7}$$

The HI absorption spectrum is given by $\tau_j(\mathrm{v})$ or sometimes plotted as $e^{-\tau_j(\mathrm{v})}$.

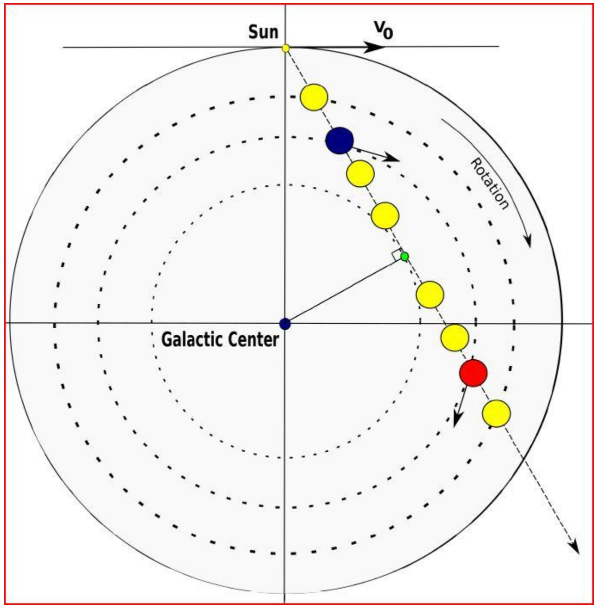

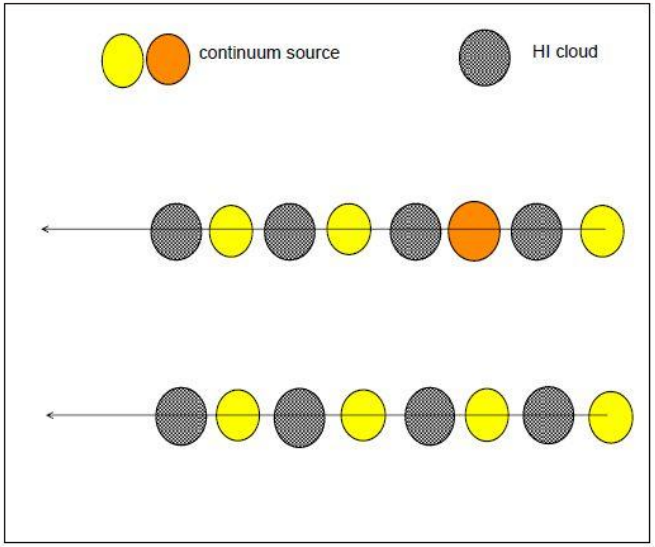

Examples of SNR images and derived HI spectra

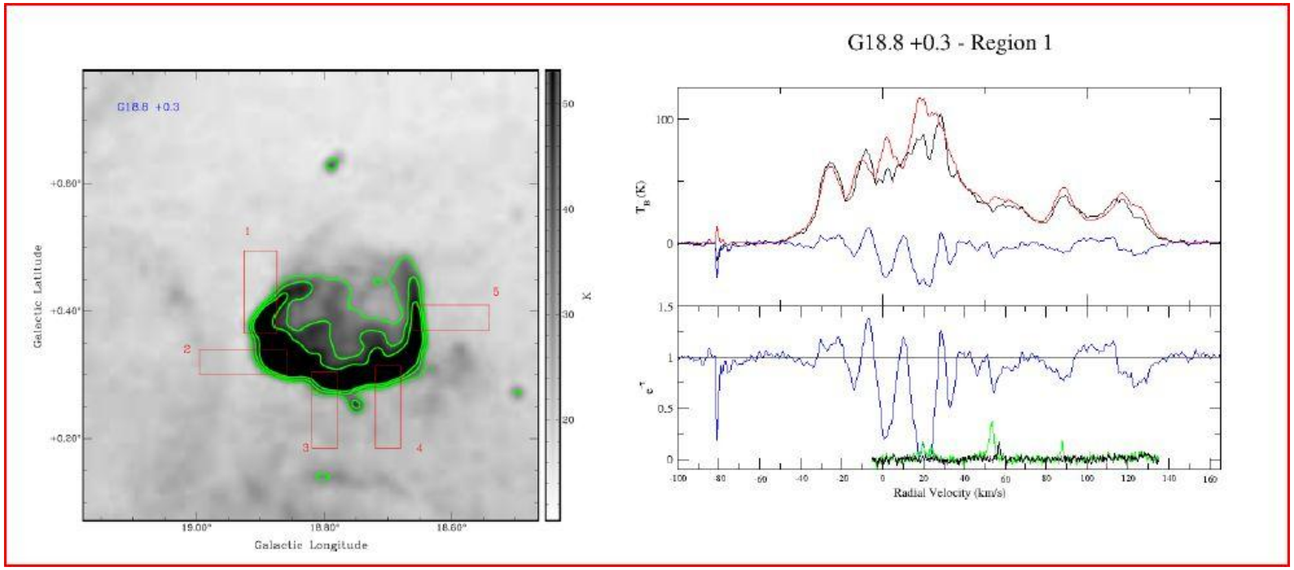

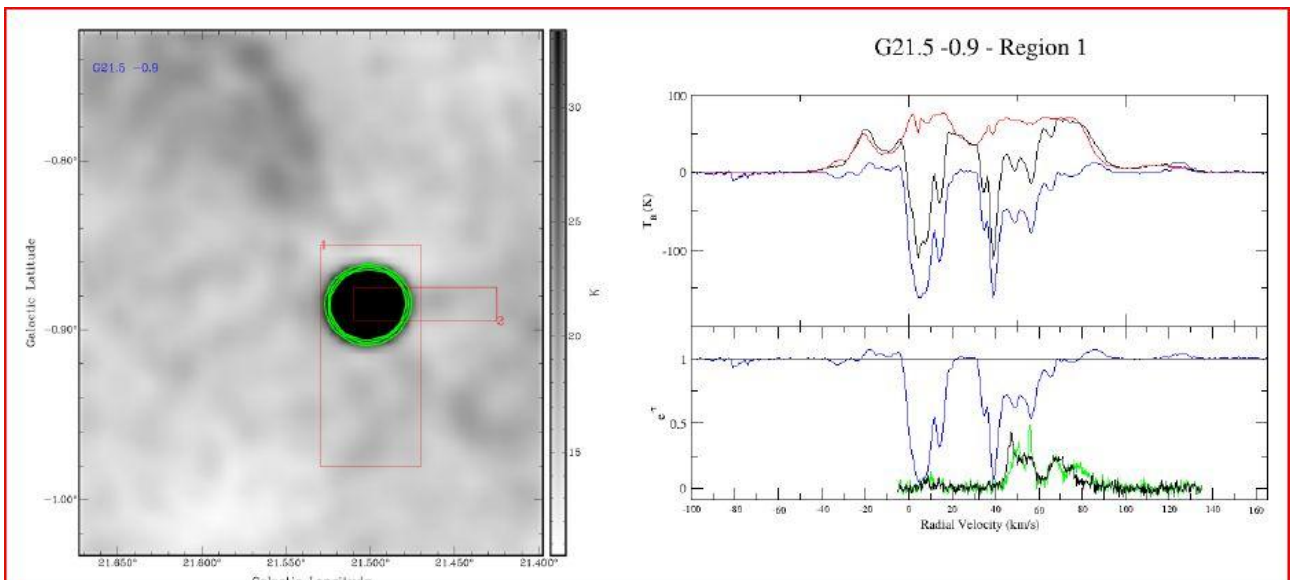

Examples of SNR images and derived HI spectra

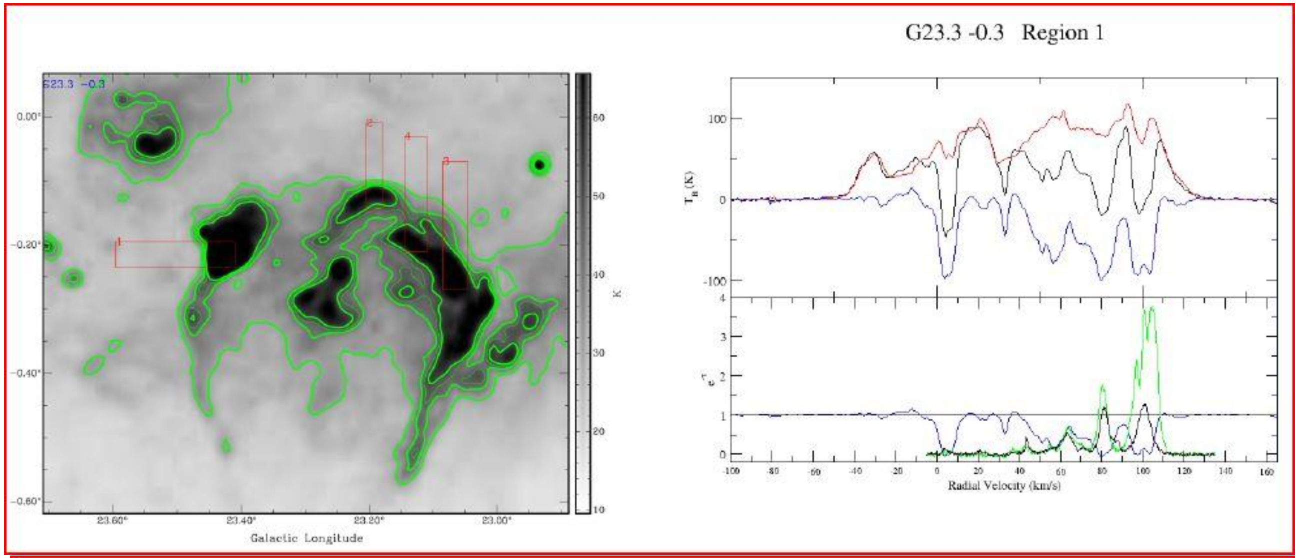

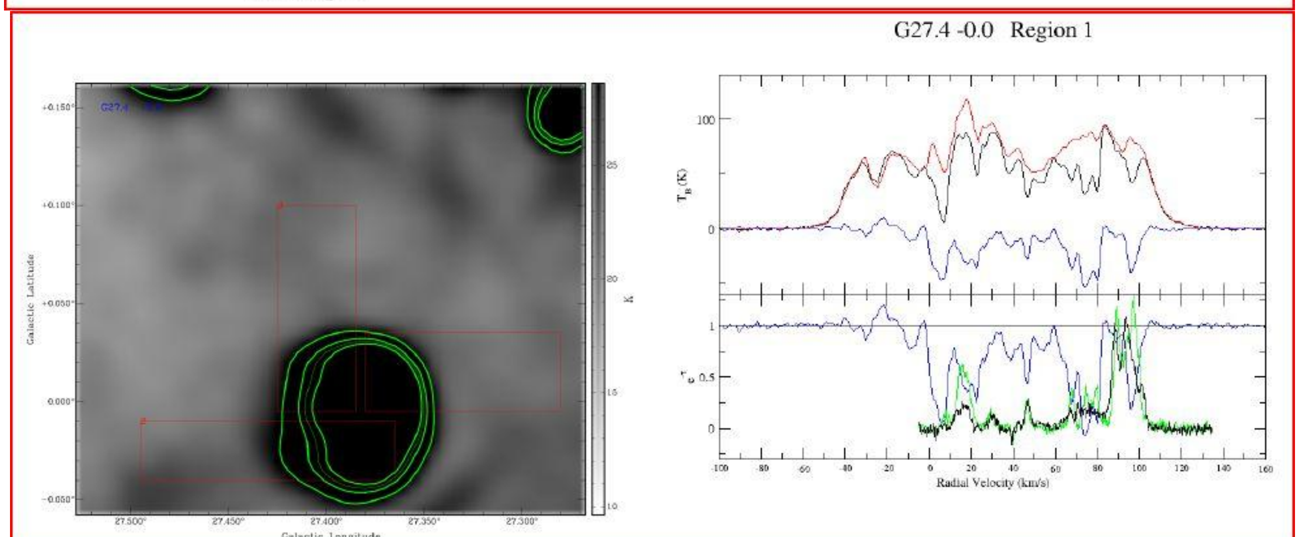

Examples of SNR images and derived HI spectra